Conference Paper, Published Version

de Almeida, E.; Hofland, B.; Jonkman, S. J.

Wave Impact Pressure-Impulse on Vertical Structures with Overhangs

Wave Impact Pressure-Impulse on Vertical Structures with Overhangs

E. de Almeida, B. Hofland & S. J. Jonkman
Delft University of Technology, Delft, The Netherlands

Abstract: The study of wave impact physics and magnitudes are key for the design of vertical coastal hydraulic structures. This research addresses the study of standing wave impacts on vertical coastal hydraulic structures with a relatively short horizontal overhang, which is especially relevant for structures such as lock gates, sluice gates, dewatering sluices, flood gates and storm surge barriers. This paper applies the pressure-impulse theory to predict the pressure-impulse caused by standing wave impacts. These theoretical estimates are compared with results from four extensive regular wave tests from laboratory experiments conducted at the Hydraulic Engineering Laboratory of the Delft University of Technology. The agreement for two test cases is good, while differences are observed in the other two cases. This study concludes that a prediction method based on the pressure-impulse theory will allow to carry out preliminary load estimations from standing wave impacts on vertical structures with overhangs. Nevertheless, further research is required considering a larger range of structure dimensions, incident wave characteristics and influencing processes such as air entrapment.

Keywords: wave impacts, vertical walls, coastal structures, hydraulic structures, overhangs, pressure-impulse theory, physical modelling

1 Introduction

In the coming years, various new hydraulic structures will be constructed around the world. Also, several existing structures will be renovated after reaching the end of the envisaged design lifetime or due to a rise in the safety standards and/or due to an increase in the loading conditions. This requires extended knowledge on the design of coastal hydraulic structures subjected to wave impacts. On the basis of wave impacts, three basic configurations can be distinguished, as shown in Fig. 1:

- Vertical wall, subjected to wave impacts caused by breaking waves.
- Overhang, subjected to wave impacts caused by standing waves.
- Crest wall, subjected to wave impacts caused by overtopping of waves.
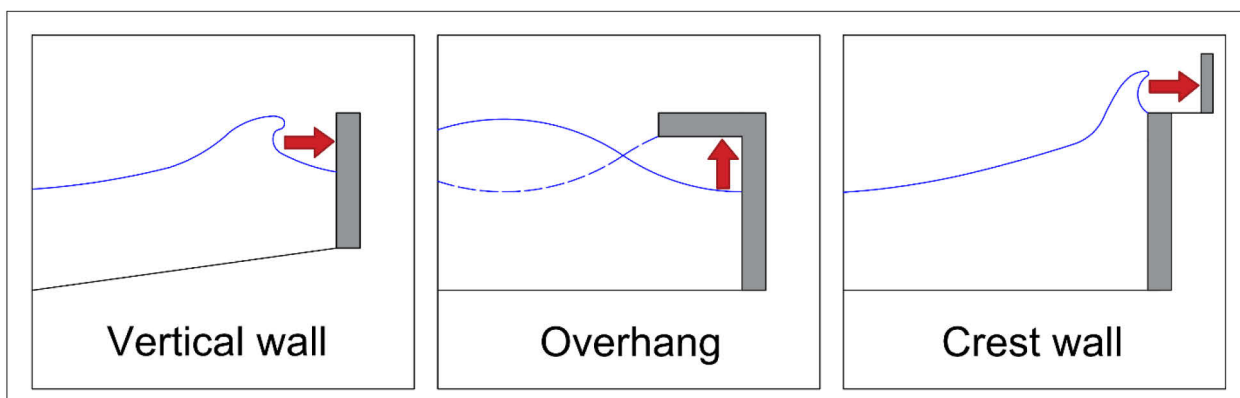

Fig. 1.   Wave impact configurations

Previous research has focused mainly on the first type of wave impacts caused by breaking waves (Goda, 1974; Goda, 2010; Oumeraci et al., 2001, Cuomo et al., 2010). In addition, wave impacts caused by overtopping waves have been studied in the last years (Chen et al., 2015, Chen et al., 2016). In contrast, a significant knowledge gap exists on wave impacts caused by standing waves, to which hydraulic structures such as lock gates, sluice gates, dewatering sluices, flood gates and storm surge barriers are exposed. This study addresses the knowledge gap on wave impacts caused by standing waves on a vertical structure with a relatively small overhang and on a flat bottom.

Fig. 2 shows a cross-section of a flood gate in the Afsluitdijk (situated in the north of The Netherlands). These flood gates remain open during low tide allowing the water to flow out from the lake to the sea. During high tide and storms, these flood gates remain closed to avoid the flooding of the hinterland. In front of the gates, both from the sea side and from the lake side, a horizontal overhang is present. In such structures, the vertically upwards moving standing wave surface at the vertical wall produces violent impacts when hitting the rigid horizontal lower overhang surface. Thus, this structure represents an example of conditions where standing waves can lead to violent wave impacts. Nevertheless, many other examples of coastal hydraulic structures with overhangs can be found, such as crest walls, lock gates, sluice gates, dewatering sluices, flood gates and storm surge barriers (Ramkema, 1978).
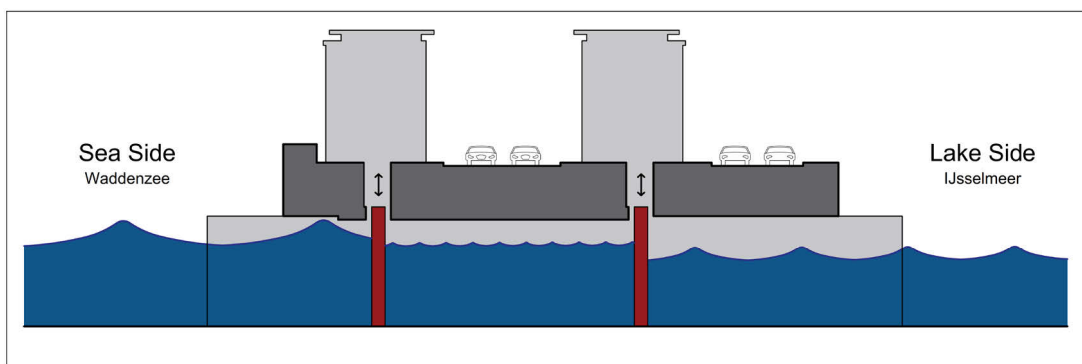
Fig. 2.   Impression of an existing flood gate complex in the Afsluitdijk (The Netherlands), with the 2 flood gates closed during high water level at the sea side (Waddenzee).

In Fig. 3 the main hydraulic and structural parameters to be considered in wave impacts on vertical structures with an overhang are shown. This paper focusses on the study of relatively small overhangs, with ratios of overhang length (W) to deep water wave length (L_0) in the range of $W/L_0 < 0.1$, and ratios of overhang height (h) and overhang length (W) in the range of $3 < h/W < 6$. This paper presents the study carried out for this type of structure and wave impact mechanism, considering mainly the pressure-impulse theory and experimental test results.

Fig. 3.   Wave impacts on vertical hydraulic structure with an overhang. Main parameters to be considered: H (wave height), T (wave period), W (overhang width), h (overhang height), d (water depth) and Rc (freeboard).

In Section 2 the literature on wave impacts and the pressure-impulse theory is summarized. In Section 3 the theoretical pr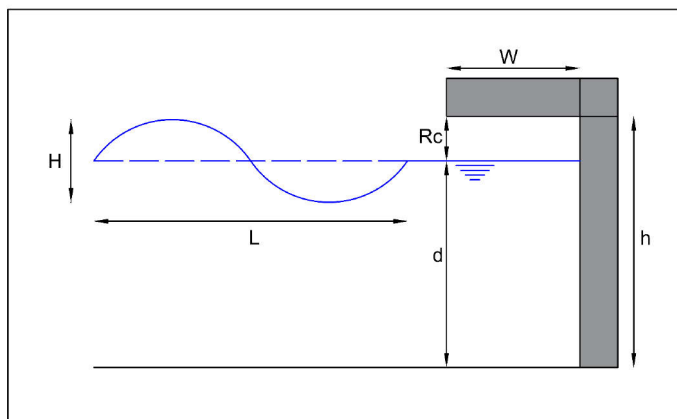essure-impulse predictions based on the pressure-impulse theory is shown, while in Section 4 the small-scale physical modelling experiments are described. Section 5 includes the comparison between theoretical predictions and laboratory measurements, while Section 6 presents the main conclusions of this study.

2 Literature

This section presents a summary of the most relevant literature taken into account in this study, which reflects the existing knowledge on wave impacts and the pressure-impulse theory.

2.1 Wave Impacts

Bagnold (1939) presented significant progress in the study of impulsive loading due to wave breaking, including two significant contributions. Firstly, the observation that although maximum peak pressures present large variations, the area enclosed by the pressure-time curve (which can be defined as pressure-impulse, as shown in Equation 1) was remarkably constant. Secondly, he contributed to the study of the effect of air in wave impact, observing the highest pressure magnitudes when the air cushion is small, but not zero. The formula by Minikin (1950), based on Bagnold's experiments, describes the occurrence of impulsive loading due to wave breaking, but was less widely used given its excessive high pressure predictions (Goda 2010).

$$P(x)_i = \int_{t_0}^{t_1} p(x,t) \cdot \mathrm{d}t \tag{1}$$

where $P(x)_i$ [Pa s] is the pressure-impulse from impact i at location x, $p(x,t)$ [Pa] is the pressure time-series during impact i at location x, t_0 [s] is start of impact i and t_1 [s] is end of impact i.

After its publication, the new set of equations presented by Goda (1974), based mainly on experimental data, has become a worldwide reference for the calculation of wave loading on vertical structures. Following the introduction of the impulsive loading coefficients by Takahashi et al. (1994), it can be used to estimate non-breaking and breaking wave pressures on vertical structures (Goda 2010). Cuomo et al. (2010) presented additional formulas based on experimental tests for vertical structures under wave breaking. Also based on experimental tests, Kisacik et al. (2014) defined formulas for vertical structures with long overhangs under wave breaking. Furthermore, large scale tests carried out in the Delta Flume at Deltares evaluated wave impact pressures at vertical walls (Hofland et al. 2010). Large scale experiments were also carried out by Bullock et al. (2007) on vertical and sloping walls. Hofland (2015) carried out tests in order to study the wave loading on the flood gates of the Afsluitdijk.

For the design of hydraulic structures Chen et al. (2019) proposed the use of pressure impulse for the design of hydraulic structures. Tieleman et al. (2019) developed a semi-analytical fluid-structure interaction model, which computes the structural response of elastic structures due to wave impacts.

2.2 Pressure-impulse theory

Cooker and Peregrine (1990, 1995) introduced the pressure-impulse theory applied to liquid impacts and wave impact conditions. This theory presents a theoretical method to estimate the wave impact magnitudes, based on the observation of Bagnold (1939) that the pressure-impulse (see Equation 1) is approximately constant. These two first contributions consider a vertical wall configuration with a horizontally moving body of water impacting on the structure (see Fig. 4a). Later on, Wood and Peregrine (1996) adapted the pressure-impulse theory to conditions where a vertically moving body of water impacts on a horizontal rigid boundary (see Fig. 4b).

a) Cooker and Peregrine (1990,1995)   b) Wood and Peregrine (1996).
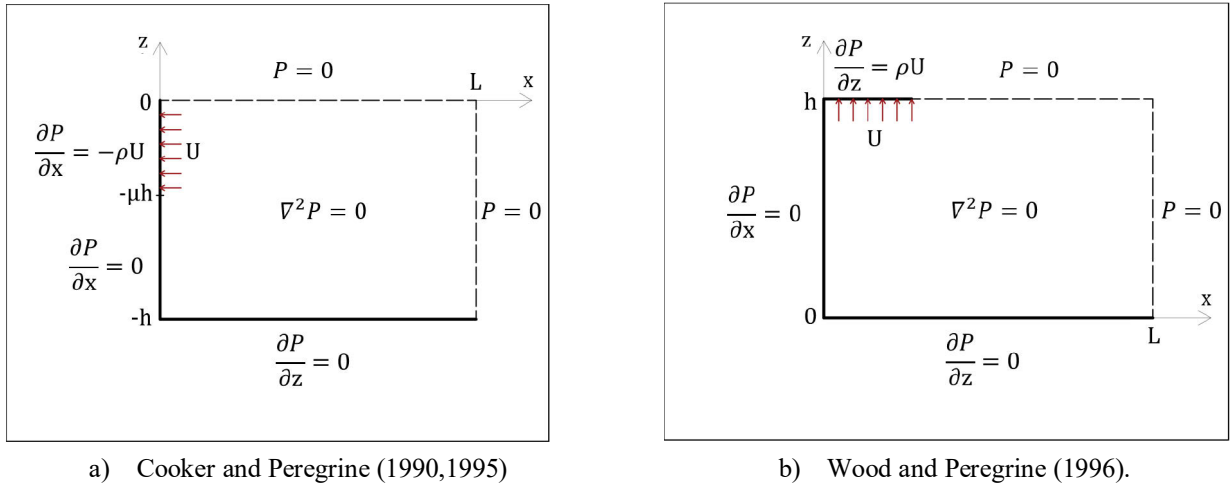
Fig. 4.   Pressure-impulse boundary conditions.

The pressure-impulse theory is based on the Navier-Stokes equation of motion, on which the viscosity and surface tension terms are considered negligible. Further, considering that the wave impact occurs in such a small period of time, the non-linear convective terms and the gravity are also neglected, which makes it possible to approximate the equation of motion to Equation 2.

$$\frac{\partial \vec{u}}{\partial t} = -\frac{1}{\rho} \nabla p \qquad\qquad (2)$$

where $\vec{u}$ [m/s] is the velocity vector, p [Pa] is the pressure and ρ [kg/m^3] is the fluid density.

The pressure-impulse concept in Equation 1 (integral of pressure over time) is considered in this theory. Since Bagnold (1939), a number of authors have observed that the pressure-impulse during wave impacts is significantly more constant than other magnitudes, such as pressure peaks. Thus, combining Equation 1 and 2, we observe that the pressure-impulse satisfies the Laplace equation (see Equation 3).

$$\nabla^2 P = 0 \qquad\qquad (3)$$

Together with the boundary conditions shown in Fig. 4 this equation can be solved to obtain the pressure-impulse distribution in the desired domain and on the vertical wall. The aim of this paper is then to compare the pressure-impulse theory predictions of wave impacts from the model of Wood and Peregrine (1996) with the results of experimental tests carried out in the wave flume.

3 Theoretical estimations

Based on the pressure-impulse theory described in the previous section, a scheme was defined in MATLAB in order to solve the Laplace equation (Equation 3) combined with the boundary conditions from Fig. 4b. In this section, the non-dimensionalization of the variables and the semi-analytical scheme are described in more detail.

3.1   Non-dimensionalization

For the study presented in this paper, the model is made dimensionless, using W (overhang length, see Fig.3) as the geometric scaling magnitude and making the upper impact boundary condition also dimensionless. The various dimensionless parameters are:
- The dimensionless overhang length ($\overline{W}$) is equal to 1.
- The dimensionless overhang height ($\overline{h}$) is equal to h/W.
- The dimensionless axes are $\bar{x} = x/W$ and $\bar{z} = z/W$.
- At the upper impact boundary: The velocity perpendicular to the solid impact boundary (y direction) varies from U before the impact to zero at the impact. Making it dimensionless by U and ρ the following boundary condition is obtained:

$$\frac{\partial P}{\partial z} = 1 \tag{4}$$

For the re-dimensionalisation of the results from the model the following conversion expressions are used for the pressure-impulse P [Pa s] obtained at any point in the fluid domain and for the total pressure-impulse I [N s/m] integrated over a given boundary such as the vertical structure below the overhang.

$$P = \bar{P} \cdot \rho \cdot U \cdot W \tag{5}$$

$$I = \bar{I} \cdot \rho \cdot U \cdot W^2 \tag{6}$$

where $^-$ represents dimensionless values, P [Pa.s] is the pressure-impulse obtained at any point in the fluid domain, I [N.s/m] is the total pressure-impulse integrated over a given boundary for one metre length, ρ [kg/m^3] is the fluid density, U [m/s] is the impact velocity and W [m] is the overhang length and the scaling factor.

3.2 Semi-analytical results

Considering the previously described expressions and boundary conditions, the problem is solved with a semi-analytical solution scheme presented by Wood and Peregrine (1996). The results at the gates are shown in Fig. 5. The results for the shorter overhang (dimensionless overhang height $\bar{h}$ equal to 6 dimensionless overhang length $\bar{W}$) are shown in Fig. 5a, while for the longer overhang (dimensionless overhang height $\bar{h}$ equal to 3 dimensionless overhang length $\bar{W}$) and shown in Fig. 5b for. The total dimensionless impulse ($\breve{I}$) is shown for both configurations in Tab. 1.

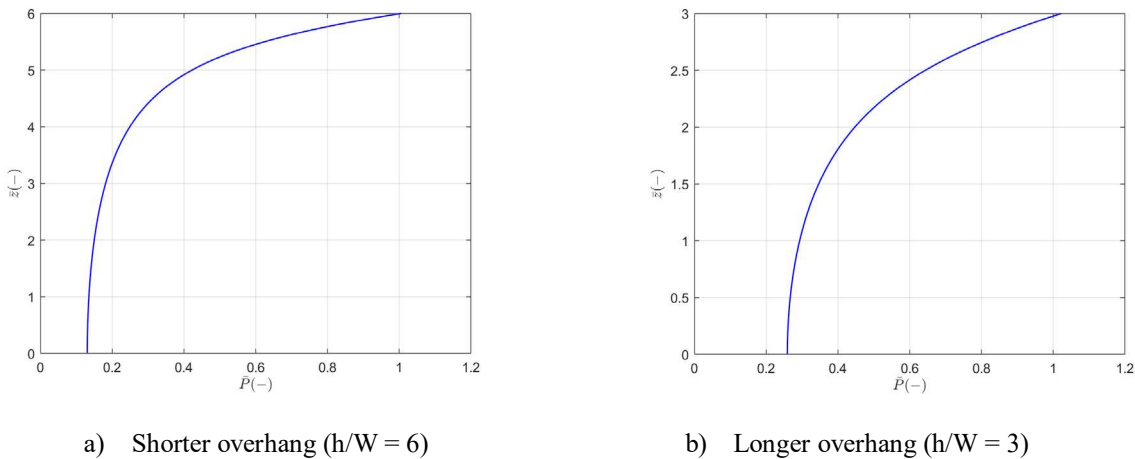| a) Shorter overhang (h/W = 6) | b) Longer overhang (h/W = 3) |

Fig. 5.   Dimensionless pressure-impulse for a wave impact over an overhang according to the pressure-impulse theory.

Tab. 1.   Dimensionless total pressure-impulse on the vertical wall

Configuration	$\bar{I}$ (-)
Shorter Overhang	1.64
Longer Overhang	1.30

4 Experimental tests

The experimental test campaign was carried out in the wave flume in the Hydraulic Engineering Laboratory (WaterLab) at the Delft University of Technology (TU Delft). Fig. 6a shows an overview of the test area, illustrating the impact structure (vertical structure with an overhang, highlighted in red) inside the green flume and connected to instrumentation and acquisition systems. Fig. 6b shows in more detail the aluminium impact surface supported by a concrete block.

a) Overview of test area   b) Model structure detail
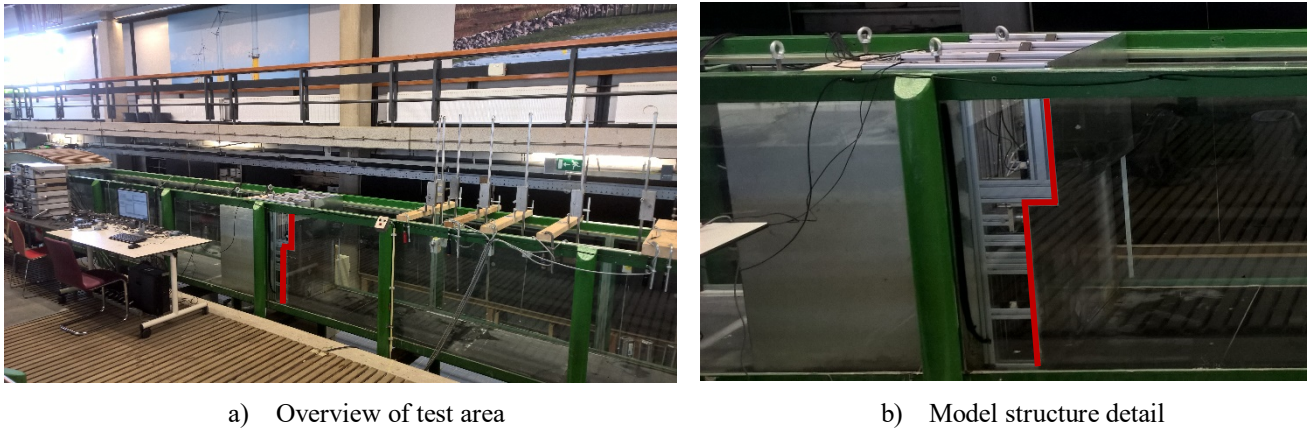
Fig. 6.   Experimental test area. a) Overview of the wave flume, impact structure (highlighted in red), instrumentation and acquisition systems. b) Detail of aluminium impact surface (highlighted in red) and concrete support block.

The wave flume is 42 m long, 1 m high and 0.8 m wide. The wave generation equipment consists of a piston-type wave maker able to generate regular and irregular waves and is equipped with active reflection compensation and second order wave steering. The use of active reflection compensation (ARC) means that the motion of the wave board compensates for the waves reflected by the structure preventing them to re-reflect back into the model. The use of second order wave steering means that second order effects of the first higher and lower harmonics are taken into account in the wave board motion. This system ensures that the generated waves resemble waves that occur in nature.

4.1   Test conditions

The test setup was built with an aluminium structure mounted on a large concrete block inside the wave flume (see Fig. 6), with the vertical wall located at 30.8 m from the wave paddle. The concrete block is 0.8 m wide, 0.8 m long and 1 m high and provides the stability for the structure subjected to wave impacts. The configurations considered in this study are shown in Fig. 7, including their geometric characteristics. These conditions, where the water level is at the overhang height (freeboard $R_c = 0$ m) are chosen in this study since there are the conditions in which the wave has the maximum upward velocity when the water surface impacts on the lower surface of the overhang. The regular incident wave conditions considered in this study are shown in Fig. 8 and Tab. 2, where the measured results are also shown.
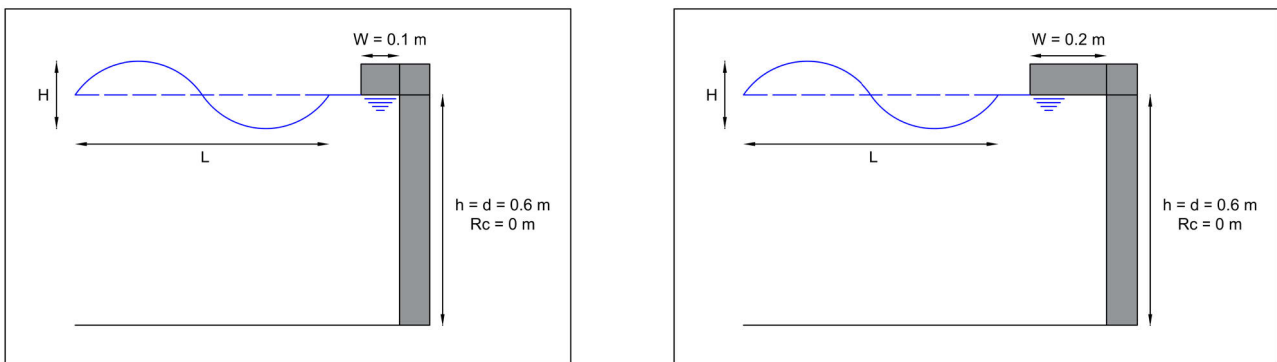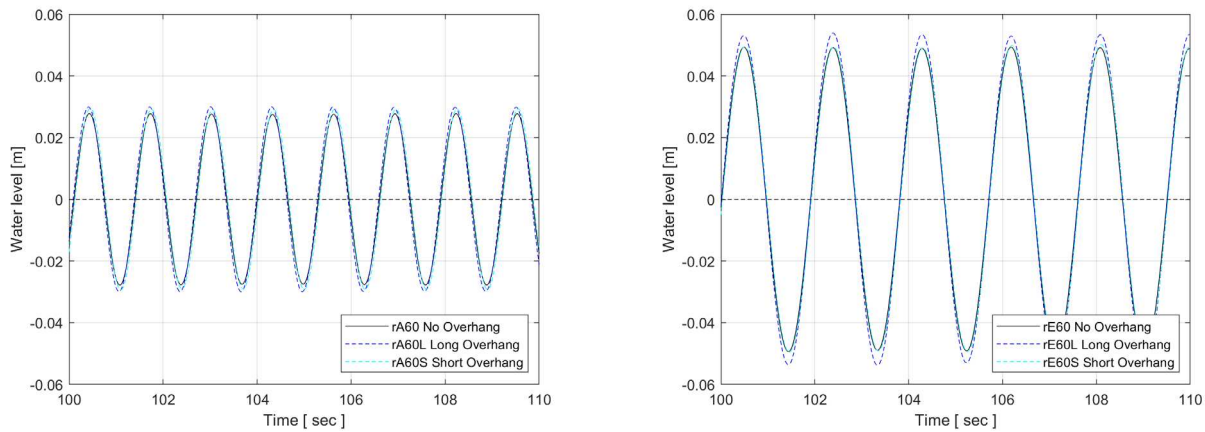

a) Shorter overhang.   b) Longer overhang.

Fig. 7.   Structure configurations.

| a) Wave condition A – smaller shorter waves. | b) Wave condition E – higher longer waves. |

Fig. 8.   Incident wave conditions.

Tab. 2.   Tested incident wave characteristics

| Configuration	Condition	Target conditions		Measured conditions	
		H (m)	T (m)	H (m)	T (m)
No overhang	A	0.06	1.3	0.056	1.3
	E	0.10	1.9	0.097	1.9
Short Overhang	AS	0.06	1.3	0.058	1.3
	ES	0.10	1.9	0.098	1.9
Long Overhang	AL	0.06	1.3	0.059	1.3
	EL	0.10	1.9	0.104	1.9

4.2   Instrumentation

In front of the structure, an array of 5 wave gauges were used to obtain the incident and reflected wave. The incident and reflected wave was determined at a location at 2.2 m from the vertical wall (see Tab. 2). In this study, the results from 7 pressure sensors are used. The pressure sensors used in the tests are Kulite HKM-375M-SG with 1 bar range and sealed gauge. The sampling frequency used was 20 kHz. The locations of these 7 pressure sensors are shown in Tab. 3, where 2 pressure sensors (PS7 and PS8) are at the same location where the maximum pressures are expected after the wave impact (the corner where the vertical wall and the overhang meet).

Tab. 3.   Pressure sensors locations

| Pressure Sensor →	PS2	PS3	PS4	PS5	PS6	PS7	PS8
Distance to the bottom (m)	0.02	0.23	0.39	0.49	0.55	0.59	0.59
Distance to the overhang (m)	0.58	0.37	0.21	0.11	0.05	0.01	0.01

4.3   Pressure-impulse estimation

The wave impact impulse from the experimental results are obtained from pairs of tests, where identical wave conditions are used for the two configurations shown in Fig. 9. Fig. 9a shows the condition where the wave is reflected from a vertical structure, registering the quasi-static wave loading, which is represented in Fig. 10a by the cyan line. In Tab. 2 these are tests A and E. Fig. 9b shows the condition where the wave impacts on the lower surface of the overhang, registering quasi-static and impulsive loading, which is represented in Fig. 10a by the blue line. In Tab. 2 these are tests AS/AL and ES/EL. Given the small difference in the incident wave conditions for the tests with and without overhangs (see Tab. 2 and Fig. 8), this study proposes that the difference between the load curves from the pairs of tests will provide the impulsive impulse (inspired by the work of Castellino et al., 2018).
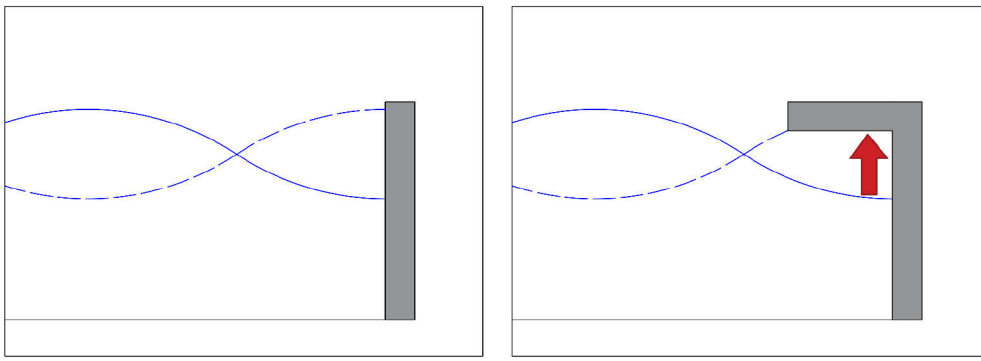
a) No overhang – quasi-static. b) With overhang – quasi-static + Impulsive.

Fig. 9.   Loading conditions in order to extract the impulse from wave impacts.
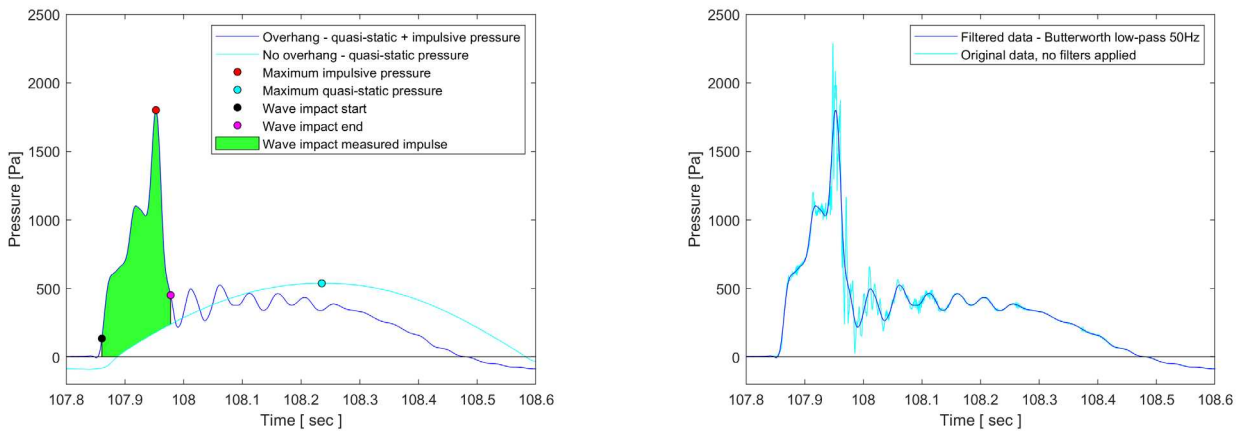
a) Wave impact impulse estimation. b) Low-pass filter effect.

Fig. 10.   Procedure for calculating the wave impact impulse, example of test AL (wave condition A, long overhang).

The original pressure data was filtered (low-pass Butterworth 3rd order filter, with cut-off frequency 50 Hz) before being used. It can be seen in Fig. 10b, that the filtering process improves the quality of the data by reducing noise, it allows a more precise estimation of the impulse with clear start and end points, and it does not affect the impulse estimations. Fig. 10a shows the process for calculating the impulse for each wave impact. For this calculation, the *difference* function is calculated as the pressures from the test with overhang/impact (blue line) minus the pressures from the test without overhang/impact (cyan line), considering only values higher than zero. The start of impact is defined when the *difference* becomes bigger than 25% of the quasi-static peak (cyan dot), while the impact end is defined when the *difference* becomes smaller than 50% of the quasi-static peak. The wave impact impulse is then calculated as the integral of the *difference* between the start and end points (green area in Fig. 10a). This process is repeated for all the waves in all the tests.

4.4   Impact velocity estimation

The impact velocity is estimated with a wave gauge placed at the vertical wall during the tests without an overhang (i.e. without impacts) as shown in Fig. 9a. From these water level measurements, the upward velocity was derived. The impact velocity is taken when the freeboard (Rc) is equal to zero and assumed to be representative for the case when the overhang is present as shown in Fig. 9b. In addition, the impact velocities derived from the linear wave theory (LWT) are also obtained and compared. These impact velocities are shown in Tab. 4.

Tab. 4.   Tested incident wave characteristics

Test name	Measured Impact Velocity (m/s)	Estimated LWT Impact Velocity (m/s)
AS	0.256 (from A)	0.28
ES	0.317 (from E)	0.32
AL	0.256 (from A)	0.29
EL	0.317 (from E)	0.34

5 Theory/experiments comparison

In this section the experimental results from the laboratory tests are compared with the theoretical estimates based on the pressure-impulse theory. The comparison of the four studied test conditions are shown in Fig. 11 (two overhang lengths and two incoming wave conditions).

The blue and green lines represent the pressure-impulse profile on the vertical wall based on the pressure-impulse theory. The blue line considers the measured impact velocity, while the green line considers the calculated impact velocity from linear wave theory. Furthermore the red line represents the mean pressure-impulse obtained from the laboratory tests (see Section 4.3 and Fig. 10a). For tests AL/AS (Fig. 11a/11b) a test period of 226 s with 173 regular waves with a period of 1.3 s are considered, while for tests EL/ES (Fig. 11c/11d) a test period of 360 s with 189 regular waves with a period of 1.9 s are considered. For the experimental results a confidence band for the mean and a prediction interval for a separate observation are shown.

It can be observed in Fig. 11, that some test conditions show better agreement than others. According to this data, the differences observed are not only related to the variations of the overhang length and incident wave condition considered in the four test conditions. This indicates that other processes have an important role in the measured loads on the wall. A possible reason for the differences between measured and estimated impulses is the entrapment of air. The entrapment of air is described as a bounce-back effect in an additional development of the pressure-impulse theory by Wood et al. (2000). This bounce-back effect caused by the presence of air pockets would increase the estimates of the pressure-impulse, and thus could partially justify the differences encountered in Fig. 11. Nevertheless, this comparison still shows the suitability of using the pressure-impulse theory for predicting the loads to be expected in standing wave impacts on vertical structures with relatively short overhangs ($W/L_0 < 0.1$ and $3 < h/W < 6$).

Tab. 5 shows the total pressure-impulse on the wall for the four tested conditions, both measured and estimated. In this case the differences on the total impulses can be quantitatively distinguished. These variations highlight once more the importance of considering other processes that affect the wave impact loading, such as the presence of air pockets.

a) AL - condition A, long overhang

b) AS - condition A, short overhang

c) EL - condition E, long overhang
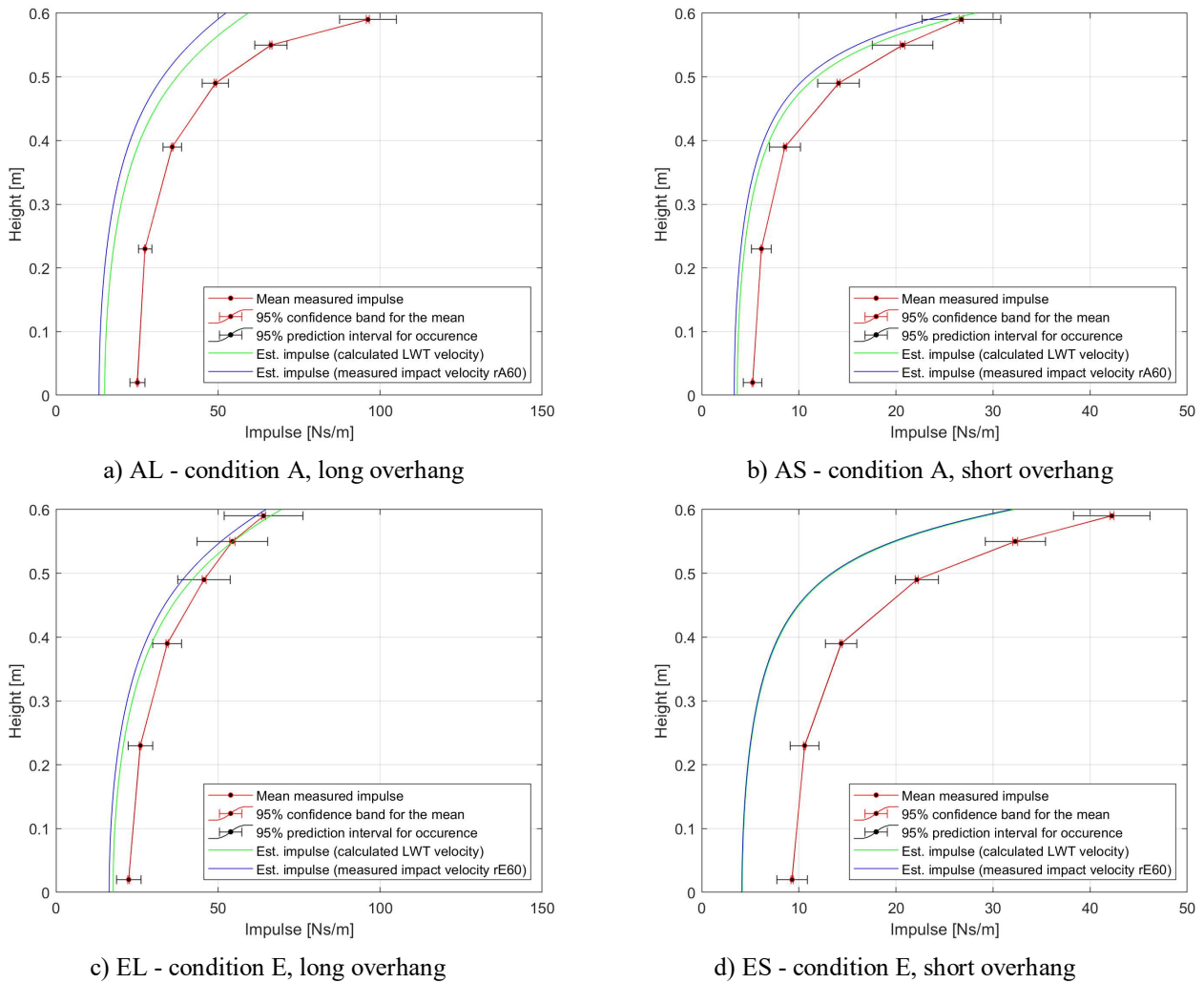

d) ES - condition E, short overhang

Fig. 11.   Estimated and measured pressure impulse. a) Test AL – Longer overhang with smaller and shorter waves. b) Test AS – Shorter overhang with smaller and shorter waves. c) Test EL – Longer overhang with higher and longer waves. d) Test ES – Shorter overhang with higher and longer waves.

Tab. 5. Tested incident wave characteristics

Test name	I (Ns/m) Measured	I (Ns/m) LWT velocity	Error (%)	I (Ns/m) Impact velocity	Error (%)
AS	5.90	4.60	-22.2	4.20	-28.8
ES	9.63	5.25	-45.5	5.20	-46.0
AL	23.09	15.13	- 34.5	13.35	-42.2
EL	20.44	17.74	-13.2	16.52	-19.2

6 Conclusions

This study addresses the loads at vertical walls caused by the impact of standing waves on rigid horizontal overhangs in front of such vertical walls. Given the various structures where such impacts can take place (crest walls, lock gates, sluice gates, dewatering sluices, flood gates and storm surge barriers), the need to bridge the knowledge gap on the prediction of such induced loads is highlighted.

This paper presents the pressure-impulse theory as a promising prediction method, however experimental validation of this theory is scarce, especially for the present configuration. With this theory, the pressure-impulse can be estimated based on the structure configuration and the impact velocity. Two methods are used for describing the impact velocity. The first is the measurement of the water surface velocity in the condition without overhang. The second is the application of the linear wave theory. Both values are in agreement for all four test conditions.

From the laboratory experiments the pressure-impulse was calculated considering tests without and with overhangs. The tests without overhangs (i.e. without impacts) are assumed to describe the quasi-static part of the load. The tests with overhangs (i.e. with impacts) are assumed to describe the same quasi-static part of the load, with the addition of the impulsive part. Thus, from the overlap of these pairs of tests the impulsive part of the load is obtained.

The comparison of the pressure-impulse estimates and the laboratory measurements leads to two conclusions. Firstly, it is considered that this method has the ability to predict the impulsive loading caused by the wave impacts. Secondly, there are differences between the predicted and measured values, which may be explained by the presence of air. It is thus important to investigate the effect of other processes present in such types of wave impacts (e.g. air entrapment and bounce back) in order to improve the applicability of this method.

Acknowledgements

References

Bagnold, R.A., 1939. Wave-pressure research. The institution of Civil Engineers, 12, 202–226.

Bullock, G., Obhrai, C., Peregrine, D., Bredmose, H., 2007. Violent breaking wave impacts. part 1: results from large scale regular wave tests on vertical and sloping walls. Coastal Engineering, Elsevier, 54 (8) 602–617.

Castellino, M., Sammarco, P., Romano, A., Martinelli, L., Ruol, P., Franco, L., De Girolamo, P., 2018. Large impulsive forces on recurved parapets under non-breaking waves. A numerical study. Coastal Engineering, Elsevier, 136 1–15.

Chen, X., Hofland, B., Altomare, C., Suzuki, T., Uijttewaal, W., 2015. Forces on a vertical wall on a dike crest due to overtopping flow. Coastal Engineering, Elsevier, 95 94–104.

Chen, X., Hofland, B., Uijttewaal, W., 2016. Maximum overtopping forces on a dike-mounted wall with a shallow foreshore. Coastal Engineering, Elsevier, 116 89–102.

Chen, X., Hofland, B., Molenaar, W., Capel, A., Van Gent, M.R.A., 2019. Use of impulses to determine the reaction force of a hydraulic structure with an overhang due to wave impact. Coastal Engineering, Elsevier, 147 75–88.

Cooker, M.J., Peregrine, D.H., 1990. A model for breaking wave impact pressures, in: Proceedings of Coastal Engineering Conference. pp. 1473–1486, Delft, The Netherlands.

Cooker, M.J., Peregrine, D.H., 1995. Pressure-impulse theory for liquid impact problems, Journal of Fluid Mechanics, Cambridge University Press, 297, 193-214.

Cuomo, G., Allsop, W., Bruce, T., Pearson, J., 2010. Breaking wave loads at vertical seawalls and breakwaters. Coastal Engineering, Elsevier, 57 (4), 424–439.

Goda, Y., 1974. A new method of wave pressure calculation for the design of composite breakwater, in: Proceedings of Coastal Engineering Conference. pp. 1702–1720, Copenhagen, Denmark.

Goda, Y., 2010. Random seas and design of maritime structures, 3rd edition. World Scientific; Singapore.

Hofland, B., Kaminski, M., Wolters, G., 2010. Large scale wave impacts on a vertical wall, in: Proceedings of Coastal Engineering Conference. pp. 1–15, Shanghai, China.

Hofland, B., 2015. Modeltesten golfkrachten spuisluizen Afsluitdijk, Deltares report. Deltares, Delft, The Netherlands.

Kisacik, D., Troch, P., Bogaert, P.V., Caspeele, R., 2014. Investigation of uplift impact forces on a vertical wall with an overhanging horizontal cantilever slab. Coastal Engineering, Elsevier, 90, 12–22.

Minikin, R.R., 1950. Winds, waves and maritime structures. Griffin; London, United Kingdom.

Oumeraci, H., Kortenhaus, A., Allsop, W., de Groot, M., Crouch, R., Vrijling, H., Voortman, H.,2001. Proverbs: Probabilistic design tools for vertical breakwaters. Balkema; Lisse, The Netherlands.

Ramkema, C., 1978. A model law for wave impacts on coastal structures, in: Proceedings of Coastal Engineering Conference. pp. 2308–2327, Hamburg, Germany.

Takahashi, S., Tanimoto, K., Shimosako, K., 1994. A proposal of impulsive pressure coefficient for design of composite breakwaters, in: Proceedings of International Conference of Hydro-Technical Engineering for Port and Harbour Construction. pp. 489–504,Yokosuka, Japan.

Tieleman, O.C., Tsouvalas, A., Hofland, B., Jonkman, S.J., 2019. A three dimensional semi-analytical model for the prediction of gate vibrations. Marine Structures, Elsevier, 65, 134–153.

Wood, D.J., Peregrine, D.H., 1996. Wave impact beneath a horizontal surface, in: Proceedings of Coastal Engineering Conference. pp. 2573–2583,Orlando, United States.

Wood, D.J., Peregrine, D.H., Bruce, T., 2000. Study of wave impact against a wall with pressure-impulse theory, I: Trapped air. Journal of Waterway, Port, Coastal and Ocean Engineering, 126 (4), 182-190.